Air Quality Modeling in the South Coast Air Basin of California: What Do the Numbers Really Mean?

Marc Carreras-Sospedra and Donald Dabdub

Computational Environmental Sciences Laboratory, The Henry Samueli School of Engineering, University of California, Irvine, CA

Marco Rodríguez

Cooperative Institute for Research in the Atmosphere, Colorado State University, Fort Collins, CO

Jacob Brouwer

Advanced Power and Energy Program, University of California, Irvine, CA

ABSTRACT

This study evaluates air quality model sensitivity to input and to model components. Simulations are performed using the California Institute of Technology (CIT) airshed model. Results show the impacts on ozone (O₃) concentration in the South Coast Air Basin (SCAB) of California because of changes in: (1) input data, including meteorological conditions (temperature, UV radiation, mixing height, and wind speed), boundary conditions, and initial conditions (ICs); and (2) model components, including advection solver and chemical mechanism. O₃ concentrations are strongly affected by meteorological conditions and, in particular, by temperature. ICs also affect O₃ concentrations, especially in the first 2 days of simulation. On the other hand, boundary conditions do not significantly affect the absolute peak O₃ concentration, although they do affect concentrations near the inflow boundaries. Moreover, predicted O₃ concentrations are impacted considerably by the chemical mechanism. In addition, dispersion of pollutants is affected by the advection routine used to calculate its transport. Comparison among CIT, California Photochemical Grid Model (CALGRID), and Urban Airshed Model air quality models suggests that differences in O₃ predictions are mainly caused by the different chemical mechanisms used. Additionally, advection solvers contribute to the differences observed among

IMPLICATIONS

Design of pollution control strategies relies on air quality simulation results. Model inputs and numerical routines are needed for air quality simulations, and the establishment of appropriate inputs and selection of numerical routines (especially the chemical mechanism) have inherent uncertainties that affect simulation results. This study quantifies the effects that changing input and model components have on $\rm O_3$ predictions for the SCAB of California. Results from this study set uncertainty bounds to simulation results. In addition, these results have implications in policy-making, because they may suggest new guidelines for assessing pollution control strategies.

model predictions. Uncertainty in predicted peak O_3 concentration suggests that air quality evaluation should not be based solely on this single value but also on trends predicted by air quality models using a number of chemical mechanisms and with an advection solver that is mass conservative.

INTRODUCTION

Regional and urban photochemical air quality models are used by regulatory agencies to design emission control strategies that lead to attainment of the National Ambient Air Quality Standards (NAAQS). However, air quality models are subject to various sources of uncertainty. Russell and Dennis¹ presented a comprehensive review on the state of the science in air quality modeling. The review identified current strengths and weaknesses of air quality models. For instance, it reported statistical errors in the prediction of O₃ and NO_x concentration by current models and presented uncertainties in input variables and model sensitivity to these inputs and emission controls. Fine et al.² identified different sources of uncertainty on air quality models and presented a compendium of techniques used for the evaluation of air quality model uncertainty and sensitivity. Both studies insist on the need for exhaustive model evaluation and intercomparison. They also emphasize the importance of reporting model uncertainty and sensitivity to advance the development of reliable air quality models.

As reported in these two studies, sensitivity and uncertainty of air quality modeling inputs have been studied in great detail by many investigators.^{3–5} In addition, there has been a tremendous effort in assessing the performance of advection solvers. Many studies used simple problems, such as transport of a puff in a rotating flow field, to assess the accuracy of the advection solution and its interaction with the atmospheric chemistry mechanism.^{6–9} Some of these studies also evaluated the effect of advection solvers on three-dimensional air quality predictions. On the other hand, there is little research on the sensitivity and uncertainty associated with changing the chemical mechanism in a full three-dimensional model. Typically, the approach is to determine the performance

of photochemical mechanisms using box model simulations. $^{10-13}$ The results in these studies are then extrapolated to the three-dimensional domain.

The main goal of this paper is to provide some insight regarding uncertainties associated with model inputs and components and to delineate the implications of such uncertainties in air quality simulation results. This study uses the California Institute of Technology (CIT) airshed model to simulate air quality in the South Coast Air Basin (SCAB) of California. The model has been validated using the meteorological episode of August 27–29, 1987. ¹⁴ The California SCAB is a region in the United States with severe $\rm O_3$ problems and where state agencies are constantly designing pollution control strategies to reach $\rm O_3$ NAAQS attainment by the year 2010. Because the year 2010 represents a special deadline in the context of air pollution control in the SCAB, this study uses emission estimates for this year to conduct the air quality simulations

The present study has three objectives to fulfill the main goal, each which is studied for the baseline year 2010 impacts using the fully detailed three-dimensional air quality model. The first objective is to quantify the effects of input variables on the uncertainty of O₃ level predictions using basic sensitivity analysis techniques. The second objective is to determine the sensitivity of predictions to changes in model components. The third objective is to compare simulation results using the CIT airshed model with predictions from the Urban Airshed Model (UAM) and California Photochemical Grid Model (CALGRID) air quality models used in the 2003 Air Quality Management Plan (AQMP). This comparison will provide insights into some of the uncertainties contained in 2010 O₃ attainment predictions performed by California state agencies.

Although the present paper addresses a well-studied topic, it contains several original contributions. This study uses the Caltech Atmospheric Chemical Mechanism (CACM), which has a comprehensive treatment of the oxidation of volatile organic compounds (VOCs) and is one of the first models to allow detailed simulation of secondary organic aerosol (SOA) formation. Simulation of SOA formation is an emerging field of study, and there have been recent advancements in model capabilities. 15,16 Results using CACM are compared with the ones obtained by the Lurmann, Coyner and Carpenter Lumped Molecule Chemical Mechanism (LCC), which assumes a more simplified chemistry. Changing the chemical mechanism in a full air quality model brings additional insights that previous studies using box models cannot provide. Previous work using the Community Multiscale Air Quality model performed a similar exercise for other regions.¹⁷ In addition, this paper is the first to address the interactions between and among changes of model components (especially the advection solver and the chemical mechanism) and model inputs through simultaneous sensitivity analyses in a full three-dimensional model in the SCAB. With this approach we hope to provide recommendations and insights that will help answer the question: what do the numbers in air quality modeling really mean?

MODEL SENSITIVITY TO INPUTS

Model simulations of an air quality episode require a series of inputs used to compute the numerical solution of the atmospheric diffusion/advection equation (eq 1). Q_m^k represents the concentration of species m in the phase k (gas phase or aerosol phase). The two terms on the left hand side of eq 1 represent the total rate of change of Q_m^k and the advective transport because of winds (denoted by u), respectively. The first term on the right side represents the transport by turbulent diffusion, where K is the eddy diffusivity tensor. The other three terms correspond with the rate of change of pollutant concentration because of sources/sinks (emissions/deposition), aerosol formation, and chemical reactions, respectively:

$$\frac{\partial Q_m^k}{\partial t} + \nabla \cdot (uQ_m^k) = \nabla \cdot (K\nabla Q_m^k) + \left(\frac{Q_m^k}{\partial t}\right)_{\text{sources/sinks}} + \left(\frac{Q_m^k}{\partial t}\right)_{\text{aerosol}} + \left(\frac{Q_m^k}{\partial t}\right)_{\text{chemistry}} \tag{1}$$

For instance, a numerical simulation relies on adequate meteorological input and initial and boundary conditions specification. Meteorological parameters that are considered in this study include temperature, solar radiation, three-dimensional wind fields, and mixing height.

Meteorological Conditions

The Southern California Air Quality Study (SCAQS) was a comprehensive campaign of atmospheric measurements that took place in the California SCAB during August 27-29, 1987. The study collected an extensive set of meteorological and air quality data that has been widely used to validate air quality models. 14,18-21 Temporal and spatial distribution of temperature, humidity, and three-dimensional wind profiles were obtained during SCAQS. These measurements are the basis for a complete set of gridded meteorological data used in air quality simulations. Zeldin et al.22 conducted an assessment of how representative the meteorological and air quality data for the 1987 SCAQS is of a typical episode. Zeldin et al.²² found that August 28, 1987, represents a "reasonable central metclass tendency," which makes it suitable for modeling. In addition, the August 27–28, 1987, episode is statistically within the top 10% of severe O₃-forming meteorological conditions.²³ Furthermore, this episode is also used by the South Coast Air Quality Management District (SCAQMD) of California to show that air pollution control strategies proposed in the AQMP 2003²⁴ will lead to O₃ attainment by 2010. Hence, this episode is used herein as the basis to evaluate model sensitivity to meteorological conditions.

The typical direction of dominant winds in the SCAB is from west to east during the day. The San Gabriel and San Bernardino Mountains form a natural barrier that enhances accumulation of air pollutants in downwind locations, such as Riverside and San Bernardino. In addition, warm and sunny summer conditions with a lack of natural scavenging processes, such as rain, favor the formation of photochemical smog and O_3 .

The SCAQS episode of August 27–29, 1987, is characterized by a weak onshore pressure gradient and warming

temperatures aloft. The wind flow is characterized by a sea breeze during the day and a weak land-mountain breeze at night. The presence of a well-defined diurnal inversion layer at the top of neutral and unstable layers near the surface and a slightly stable nocturnal boundary layer facilitated the accumulation of pollutants over the SCAB and lead to an episode of high $\rm O_3$ concentration.

Temperature. O_3 concentration is affected by temperature because of the strong temperature dependence of peroxyacetyl nitrate (PAN) decomposition. High temperatures favor PAN decomposition, thus increasing NO_x, which is an O₃ precursor.^{25,26} Sillman and Samson²⁶ suggest that increased temperatures are correlated to higher biogenic VOC emissions and higher UV radiation, which could contribute to enhanced O₃ formation. They also suggest that high temperatures might be correlated with higher anthropogenic emissions and stagnant circulation conditions. Bärtsch-Ritter et al.²⁵ studied the effects of meteorological conditions on the air quality of Milan, Italy. Based on simulation results, that study showed that increasing temperature leads to an increase of the total area under a VOC-limited regime, mostly because of lower PAN formation. A VOC-limited regime is one where nitric acid formation, which terminates the O₃ photochemical cycle, prevails over the NO_X-O₃ recycling through VOC oxidation. If VOC-limited areas increase, O₃ concentrations are less sensitive to changes in NO_X emissions and concentrations. Therefore, temperature is potentially an important factor in the design of an air pollution control

During August 27–29, 1987, temperatures ranged from moderate at night (\sim 15–20 °C) to high at downwind locations in the early afternoon (maximum temperature: 42 °C). Various simulations are performed with the model in which temperature is systematically changed by -10, -5, +5, and +10 °C over baseline values. Results indicate that these changes affect peak O_3 values by \sim 6 ppb/°C. Maximum changes in O_3 concentration reach values \leq 10 ppb/°C.

Note that the simulations performed are numerical experiments in which only temperature is changed. As suggested by previous studies, an increase in temperature leads to increased biogenic and anthropogenic emissions and could create more stagnant conditions and intense insolation. These combined effects could lead to even more significant impacts than those reported here, because the emissions and all of the meteorological parameters except temperature were not changed. This method of sensitivity analysis allows for a careful characterization of how the modeled concentrations are affected by changes in temperature alone.

UV Radiation. O_3 formation depends on NO_2 photolysis by UV radiation. Harley et al.³ described that solar UV radiometers operated at five locations in the SCAB during the August 27–29, 1987, episode. These measurements of UV irradiance are used to obtain NO_2 photolysis rates. Additionally, "clear sky" photolysis rates can be obtained as a function of the solar actinic flux, which is a function of the solar zenith angle, the elevation, and the wavelength. In the baseline simulation, UV scaling factors are

calculated as the ratio of actual photolysis rates to clear sky values for each monitoring station. These scaling factors are calculated at each hour and extrapolated for the rest of the domain. Typical UV scaling factors at midday for this episode are 1 for Central Los Angeles, 0.8 for Claremont, 0.65 at Rubidoux, and 1.2 for Mount Wilson. Harley et al.³ compared baseline simulation results, obtained by using UV scaling factors that accounted for light scattering, with simulations considering only clear sky photolysis rates. In the latter scenario, in which UV radiation is incremented by \leq 50% with respect to the baseline in areas such as Rubidoux, O_3 concentrations increased by 10–30 ppb.

For the present study, UV radiation is scaled by factors of 0.8 and 1.2 throughout the basin at all times. Simulation results show that maximum changes in $\rm O_3$ concentrations and changes in the basin-wide peak $\rm O_3$ concentration are 1 ppb per 1% change in UV radiation. These results are comparable to those obtained by Harley et al.³

Vuilleumier et al. 27 studied the factors that contribute to UV optical depth in the Los Angeles area. Results from the study suggested that light scattering and absorption are responsible for $\leq 90\%$ of the reduction in actinic flux (UV optical depth). A secondary factor is light absorption by O_3 , which, under typical SCAB conditions, contributed $\leq 10\%$ of the reduction in the actinic flux. These results imply that changes in O_3 and aerosol concentrations could have a feedback effect on the UV scaling factor. Thus, the sensitivity of 1 ppb of O_3 per 1% change in UV radiation determined herein could be reduced by this feedback effect.

Mixing Height. The height of the mixing layer determines the vertical dispersion of pollutants. During the SCAQS episode, upper air soundings were performed in 8 sites that covered coastal and inland regions.³ Mixing heights were derived from potential temperature plots obtained from the upper air measurements. During the episode, a well-defined inversion layer developed on the top of neutral/unstable layers close to the surface. Mixing heights ranged from ~50 m at night to 1100 m in the afternoon.

Previous studies have evaluated the impact of mixing height on pollutant concentrations. Harley et al.3 simulated the 1987 SCAQS episode and doubled the mixing height, which resulted in small incremental changes in O₃ concentrations. Other studies focused on the effect of mixing height on pollution control strategies. Sistla et al.²⁸ evaluated control strategies in the New York City area and compared results between using a variable mixing height versus a fixed mixing height. The study showed that to decrease O₃ concentrations it is more effective to reduce NO_x than VOC emissions if a uniform mixing height is assumed. When a variable mixing height is assumed, the control of VOC emissions is more effective. Li et al.²⁹ studied the effect of mixing heights on the efficiency of NO_X emission control toward O₃ reduction in the New York City area. The study showed that NO_x emission controls were significantly more effective when the mixing height was reduced by 50% with respect to baseline values.

In this study, the mixing height is scaled by 0.8 and 1.2 to evaluate its effect on O_3 concentrations. Although these factors are applied evenly throughout the domain during the 3 days of simulation, the model sets the minimum mixing height to 25 m and the maximum height to 1100 m. Reduction of the mixing height reduces O_3 concentrations by 30 ppb in central areas of Los Angeles and increases O_3 by 30 ppb at some downwind locations. Conversely, increasing the mixing height causes the opposite effect. However, peak O_3 concentration only decreases by 1 ppb when mixing height is reduced and decreases by 2 ppb when the mixing height is increased.

Wind Fields. Previous studies have explored the effect of wind speed on pollutant concentrations.^{3,25,30} These studies show that increasing wind speed increases the influence of the upwind boundary conditions. In the case of the Los Angeles area, upwind boundaries are typically located over the ocean, where pollutant concentrations are low. As a result, these boundaries introduce clean air that tends to dilute pollutant concentrations inside the basin. On the other hand, decreases in wind speed provide stagnant conditions that tend to accumulate air pollutants in the domain, increasing their concentrations.

Harley et al.³ reported an increase of 50 ppb in peak O₃ concentration by reducing wind speeds by 50% using wind fields from the 1987 SCAQS episode. The current study finds that peak O₃ concentration increases by 62 ppb when the same numerical experiment is conducted. This discrepancy arises from the use of different emissions inventories, chemical mechanisms, and advection solvers. On the other hand, the current study finds that increasing wind speeds by a factor of 2 decreases peak O₃ concentration by 70 ppb. In some areas, O₃ concentrations are 100 ppb lower than baseline simulation values. Furthermore, the location at which the peak O₃ occurs is also affected by the wind speed. Slower winds shift the O₃ peak closer to the main source of emissions. On the other hand, higher wind speed shifts the location of peak O₃ farther downwind.

Boundary Conditions

Interpolated values from measurements are typically used as boundary conditions for model diagnosis using historical smog episodes. In contrast, specific values of pollutant concentrations are assumed for the boundary conditions in simulations of future years. To minimize the impact of inadequate lateral boundary conditions on air quality predictions, boundaries should be located far away from the main area of study. However, the size of the domain is typically constrained by data availability and computational power.

Previous studies have tried to analyze the effect of boundary conditions on air quality simulation results. Winner et al. 31 compared O_3 isopleths from two different sets of boundary and initial conditions (ICs): the first case used interpolated values from data measured during the 1987 SCAQS episode for both boundary and ICs. The second case used clean air values for both boundary and ICs. The study found that it is not possible to reach peak

O₃ concentrations lower than the federal air quality standard (1-hr average concentration: 120 ppb) by using values based on measurements. On the other hand, the study showed that when clean air values are used, the O₃ federal air quality standard is attained by reducing reactive organic gases emissions by 50%. There are some indications, based on previous studies, that pollutant concentrations over the ocean to the west of the Los Angeles area (prevailingly upwind area) are affected by emissions from downwind onshore emissions.³² Hence, concentrations at the boundaries could be affected by a significant reduction of emissions at downwind locations. Particularly, concentrations at the boundaries tend to reach clean air conditions when continental anthropogenic emissions tend to zero.

Dabdub et al. 30 investigated the impact of boundary conditions on the air quality predictions in the San Joaquin Valley. O_3 formation in this area is not as strongly dominated by in-basin emissions as in the Los Angeles area. Hence, boundary conditions have a significant effect on air quality simulation results. Results showed that O_3 concentrations at locations near the inflow boundary (west boundary) are more sensitive to the O_3 boundary condition than to NO_X -VOC boundary conditions. On the other hand, O_3 concentrations at downwind locations, far from the inflow boundary, are more sensitive to NO_X -VOC boundary conditions.

The current study is based on the combined methodologies of Dabdub et al. 30 and Winner et al. 31 to determine the sensitivity of $\rm O_3$ concentrations to boundary conditions. Six different scenarios are simulated: (1) baseline, (2) all boundary conditions set to zero, (3) $\rm O_3$ boundary conditions set to zero, (5) VOC boundary conditions set to zero, and (6) clean air boundary conditions as described in Winner et al. 31 Table 1 presents the boundary conditions used in the simulation of cases 1 and 6. Figure 1, a–f, shows the 1-hr average $\rm O_3$ concentrations at 3:00 p.m. (when $\rm O_3$ reaches its maximum value in the baseline case) of the third day of simulation using these different boundary conditions.

All of the cases with boundary conditions set to zero are used for model diagnosis, because even in the cleanest air, concentrations of O₃, NO_X, and VOC are not zero. Case 2, all boundary conditions set to zero, shows decreases of \sim 170 ppb in O₃ concentrations over the central part of the domain because of dilution and a subsequent decrease in O₃ production caused by pollutant-free air inflow through the western boundary. Among cases 2–5, zero O₃, NO_x, and VOC boundary conditions, respectively, case 5 leads to the largest decrease in O₃ concentrations in the central part of the basin. Furthermore, setting the VOC boundary condition to zero leads to the largest decrease in domain-wide 1-hr peak O₃ concentration (5 ppb smaller with respect to the baseline case). On the other hand, setting the NO_x boundary condition to zero leads to an increase of 1 ppb in 1-hr peak O3 concentration. These results confirm that O₃ formation in Los Angeles is VOC limited. O₃ boundary conditions set to zero lead to decreases of 100 ppb with respect to the base case in the central part of the domain, although peak O₃

Table 1. Boundary conditions used for the simulation of the base case and the clean air case (in ppb).

Species	Boundary	Baseline Case Vertical Layer in Model				Clean Air Case Vertical Layer in Model					
		Surface	Lev 2	Lev 3	Lev 4	Lev 5	Surface	Lev 2	Lev 3	Lev 4	Lev 5
NO_2	N, S, W	1	1	1	1	1	1	1	1	1	1
NO_2	E	aq	aq	1	1	1	1	1	1	1	1
NO	N, S, W	1	1	1	1	1	1	1	1	1	1
NO	E	aq	aq	1	1	1	1	1	1	1	1
0_3	N	aq	70	70	70	60	40	40	40	40	40
03	E	aq	aq	60	70	70	40	40	40	40	40
03	S, W	40	40	40	40	40	40	40	40	40	40
RHC	N	aq	100	100	100	100	10	10	10	10	10
RHC	Е	aq	aq	100	100	100	10	10	10	10	10
RHC	S, W	100	100	100	100	100	10	10	10	10	10
HCH0	N, E	aq	aq	3	3	3	3	3	3	3	3
HCH0	S, W	3	3	3	3	3	3	3	3	3	3
ALD2	N, E	aq	aq	5	5	5	5	5	5	5	5
ALD2	S, W	5	5	5	5	5	5	5	5	5	5
MEK	N, E	aq	aq	4	4	4	4	4	4	4	4
MEK	S, W	4	4	4	4	4	4	4	4	4	4
CO	N, E	aq	200	200	200	200	120	120	120	120	120
CO	S, W	200	200	200	200	200	120	120	120	120	120

Notes: Lev = level; N = N north; S = N south; E = N west; E = N

concentration remains unchanged. As mentioned earlier, locations near the west boundary, with a net inflow to the basin, are affected by boundary conditions more than downwind locations located closer to the eastern boundary. Finally, case 6, clean air boundary conditions, produces a decrease in the $\rm O_3$ peak of 1 ppb and reductions in $\rm O_3$ concentration over the central area on the order of 30 ppb.

ICs

Previous work assumed that simulations of 2-day episodes are sufficient to minimize the effect of ICs on air quality modeling. 18,24,31 Additionally, the simulation of longer episodes is limited by data availability. This section presents the effect of ICs on air quality predictions. Two simulations are conducted: (1) a 10-day episode using the baseline ICs, and (2) a 10-day episode with zero ICs for all species. Because there are no data for an episode that extends for 10 consecutive days, meteorological conditions used from days 3 to 10 are identical to those of day 2. Because the meteorology, emissions, and boundary conditions are equal for the third and subsequent days, it is expected that pollutant concentrations reach a stationary cycle after a given number of days of simulation. Also, pollutant concentrations in the case of zero ICs will be closer to those of the base case as time progresses.

Figure 2 presents the evolution of O_3 at six different locations, for the two cases studied: baseline and zero IC cases. Figure 2, a and b, shows O_3 concentrations in Central Los Angeles and Long Beach, respectively. These two sites represent upwind locations strongly dominated by direct emissions. As a result, O_3 concentration in the zero IC case recovers, with respect to the baseline case, by the second day of simulation. Figure 2, c and d, shows O_3

concentrations in Riverside and San Bernardino, respectively. These two cities are located at downwind locations, and although they have an important contribution from local emissions, the air quality in this region is dominated by transport of pollutants from the central area of Los Angeles. Because local emissions are not as important as in the previous upwind cities, O3 concentrations in the zero IC case need 2 days to reach the values of the baseline case. This result is particularly important, because maximum O₃ concentrations are usually found over these regions, and air pollution control strategies are designed based on peak concentrations. Figure 2e shows O₃ in Hesperia, a location close to the northeastern boundary where the maximum O₃ concentrations are predicted, and Figure 2f shows O₃ in Palm Springs, which is located far downwind from Los Angeles and from other major anthropogenic emissions. For these two locations, the recovering time for O₃ concentrations in the zero IC case with respect to the baseline case is 3 days. In short, the farther a location is from the central area, where major emissions occur, the more lasting the effects of the ICs are. This suggests that control strategies for the SCAB should be based on simulations of ≥ 3 days to minimize the impact of ICs over the areas where O_3 concentrations are the highest.

SENSITIVITY TO MODEL FORMULATION

The preceding section focuses on model sensitivity to various inputs. The approach used here consists of analyzing the impacts on O_3 concentration because of parametric changes in input variables. This section, on the other hand, focuses on model sensitivity to model components. Determination of model sensitivity to structural changes and to model formulation is more challenging.

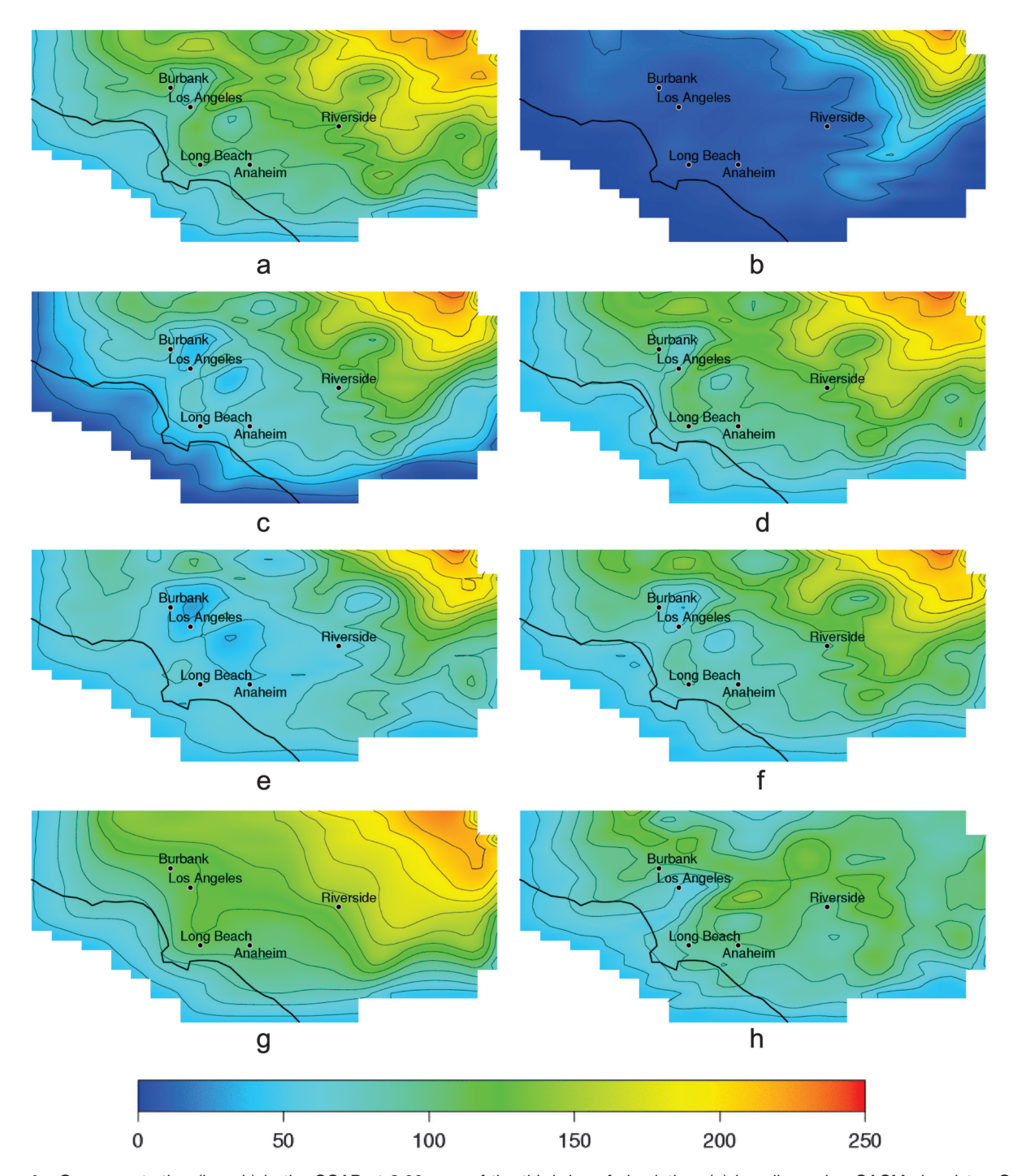


Figure 1. O_3 concentration (in ppb) in the SCAB at 3:00 p.m. of the third day of simulation. (a) baseline using CACM chemistry, QSTSE advection solver, and baseline boundary conditions as shown in Table 1; (b) zero all boundary conditions; (c) zero O_3 boundary conditions; (d) zero O_3 boundary conditions; (e) zero volatile organic compound boundary conditions; (f) clean air boundary conditions; (g) using Galerkin advection solver; (h) using LCC chemical mechanism.

Traditionally, differences among model predictions have been explained on the basis of direct model-to-model comparison and community expertise.² In addition, to reduce computational expenses, sensitivity analyses of model structure are often assessed with zero-dimensional and one-dimensional models as a first approximation to more complex three-dimensional models. The present work uses a full three-dimensional model to directly assess sensitivity to model formulation.

Advection Solver

Advection is one of the processes included in the atmospheric diffusion equation (eq 1), which is solved by operator splitting schemes. Previous studies have evaluated the effect of the advection solver algorithm on air quality modeling. Chock³³ and Dabdub and Seinfeld⁷ reported that the Accurate Space Derivative (ASD) scheme is the best algorithm in terms of peak preservation properties, mass conservation, and average absolute error (difference

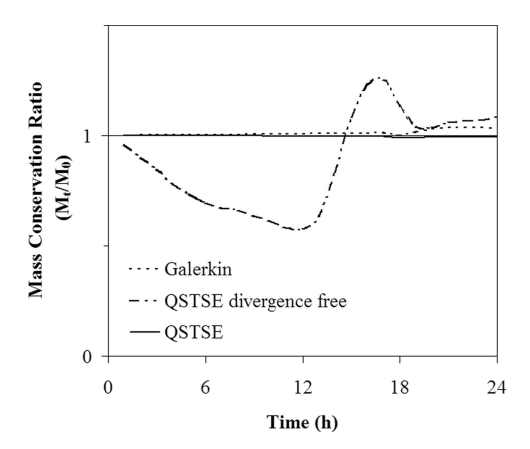


Figure 2. Evolution of O_3 concentration (in ppb) at six different locations during 4 days of simulation: baseline case in solid line; zero ICs case in dashed line.

between numerical and analytical solution). Dabdub and Seinfeld⁷ also reported that the finite-element Galerkin solver was the second-best advection scheme and significantly less CPU-intensive than the ASD method. According to various studies, the Smolarkiewicz method, which is used for $\rm O_3$ attainment demonstration with the UAM model, 34 produces the least accurate results, and those researchers suggest using other methods for air quality modeling. 7,8,35 The Galerkin scheme is used with the CALGRID model for the SCAQMD 2003 Air Quality Management Plan to support $\rm O_3$ attainment demonstration by the UAM model. 24

Nguyen and Dabdub9 formulated an advection solver, Quintic Spline Taylor-Series Expansion (QSTSE), that is comparable to the Galerkin scheme in terms of CPU expense, but it improves predicted peak O₃ concentrations in a full model by 27.5%. QSTSE is significantly faster than ASD and produces similar peak retention, is mass conservative, and is positive definite. Figure 1, a and g, shows O₃ concentration at hour 15 using the QSTSE and Galerkin schemes, respectively. Both advection solvers show that the O_3 peak is located over the same area. The maximum O₃ concentration predicted by the Galerkin scheme is 246 ppb, which is 12 ppb lower than the one predicted by QSTSE. On the other hand, the Galerkin scheme produces O_3 concentrations ≤ 80 ppb larger than QSTSE. The QSTSE algorithm estimates a less diffusive solution of the advection equation than Galerkin. Furthermore, QSTSE has better peak retention than the Galerkin scheme. These results show that higher peak retention does not imply higher predicted O₃ concentrations. Because peak retention affects all species equally, including NO_X, O₃ destruction may be enhanced. NO_X concentration is diffused more strongly by Galerkin than by QSTSE, and because Los Angeles is typically under a VOC-limited regime, O₃ concentrations predicted by Galerkin in this area are higher than the values predicted by QSTSE.

Mass Conservation. One important quality that determines the accuracy of an advection solver is its ability to conserve mass. Previous studies have assessed mass conservation of the advection solvers mentioned above.^{7,9,33} According to Nguyen and Dabdub,⁹ QSTSE, ASD, and

Galerkin advection solvers achieve mass conservation in the simulation of a rotating cosine hill after two revolutions. This test enables assessment of mass conservation in a divergence-free field. Typically, urban air quality models assume that the atmosphere has constant density. Consequently, these models require divergence-free wind fields so that mass conservation can be imposed from the continuity equation. However, wind fields obtained from meteorological data usually include a residual divergence that has to be minimized. Nguyen and Dabdub⁹ tested various advection schemes in a divergent field and found that QSTSE conserves mass satisfactorily under such conditions. Galerkin and ASD advection solvers showed mass losses of 6 and 36%, respectively.

Application of any advection solver in an air quality model has to consider and account for the inevitable residual divergence in wind fields. From the advection equation (eq 2), the term $\nabla \cdot u$ must be accurately determined, unless the wind field is completely divergence free (eq 3). Dismissing this term when the wind field is slightly divergent may dramatically impact mass conservation of the algorithm.

$$-\frac{\partial c}{\partial t} = \nabla \cdot (uc) = u \cdot \nabla c + c \nabla \cdot u \tag{2}$$

$$-\frac{\partial c}{\partial t} = u \cdot \nabla c \tag{3}$$

Figure 3 shows the normalized mass of a puff as a function of time as it is transported throughout the CIT airshed domain. The puff is located initially over Long Beach and has a parabolic shape: $c = 100 (1 - [R/4]^2)$, where R is the radius of the puff in cell units. August 27, 1987, meteorological data is used for this experiment. No sinks or sources of any kind, such as chemical production or loss, deposition, or emissions, are considered. Three cases are simulated, each containing a different advection solution algorithm: (1) Galerkin, (2) QSTSE, and (3) QSTSE, assuming $\nabla \cdot u = 0$. Results show that QSTSE is the scheme with the best mass conservation. The Galerkin scheme also performs well during the first hours. However, at hour 18, it starts adding mass into the system. This mass comes from the numerical filter that has to compensate for the negative concentrations generated by the numerical solution of the advection equation. Because QSTSE is positive definite, no filter is needed. The problem with divergent wind fields arises if the term $\nabla \cdot u$ is assumed to be zero. As Figure 3 depicts, assuming divergence-free wind fields causes the total mass to decrease dramatically during the first hours and later to increase suddenly, artificially adding mass to the system. Consequently, divergence of a wind field has to be considered, and use of the QSTSE advection algorithm is recommended to preserve mass conservation.

Chemical Mechanism

There are a large number of components in the atmosphere that undergo numerous reactions.³⁶ A chemical mechanism is an approximate representation of all the chemical processes that occur in the atmosphere and is

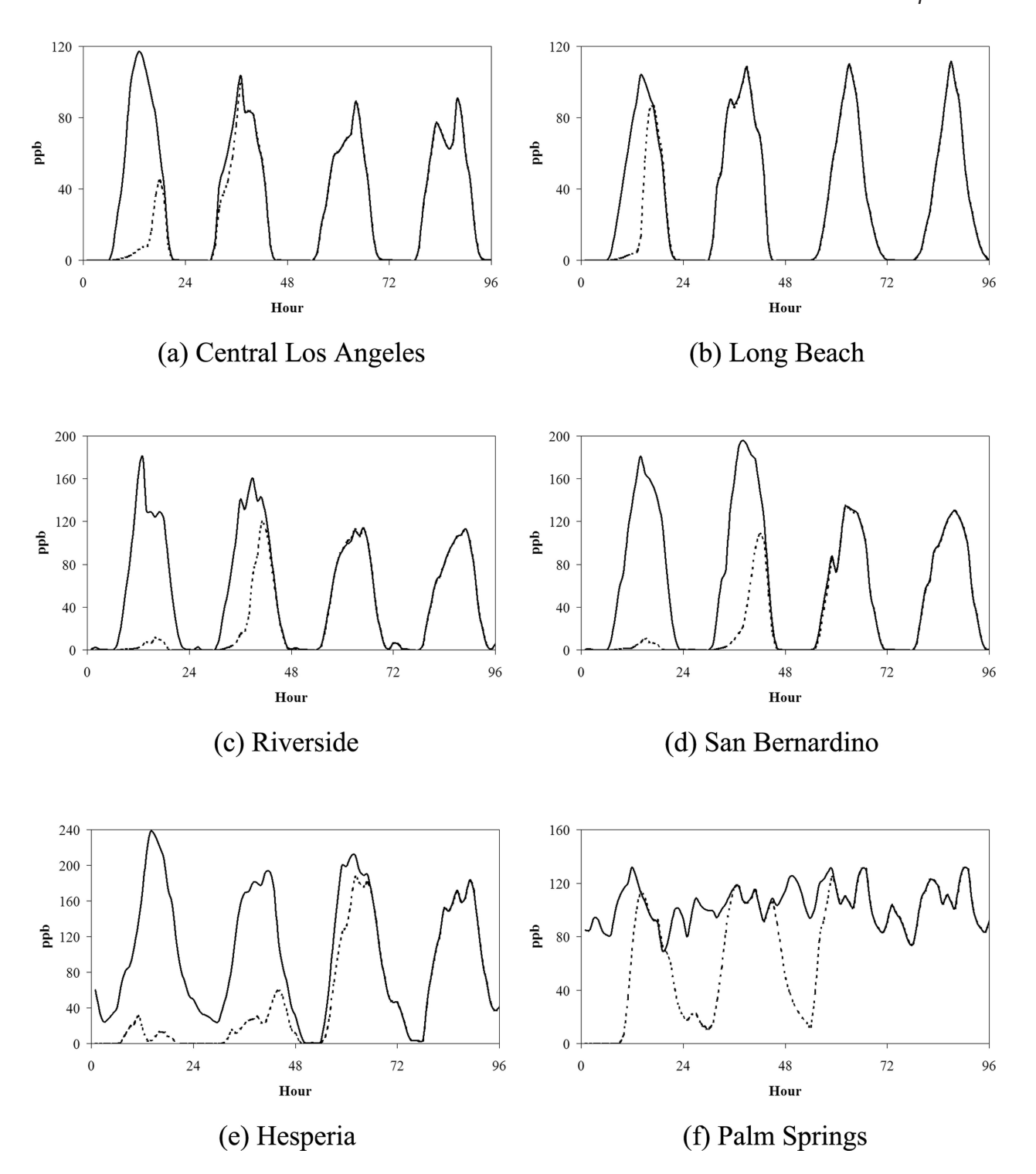


Figure 3. Mass conservation of different advection solvers applied to the CIT airshed model. Values represent the mass conservation of a puff transported throughout the domain, with no chemistry, no deposition, and no other losses.

limited by the information available for each reaction and the products that result from them. In addition, more complex chemical mechanisms may be limited by computational constraints. Russell and Dennis¹ listed the Regional Acid Deposition Model (RADM), the Regional Atmospheric Chemistry Mechanism (RACM), the Carbon Bond IV (CB-IV), and the Statewide Air Pollution Research Center model (SAPRC)-90, as the most commonly used chemical mechanisms in air quality modeling. The SAPRC model has been updated continuously to the newer versions, SAPRC-97 and SAPRC-99. Both SAPRC-99 and CB-IV are used in the SCAQMD 2003 AQMP for O₃ attainment demonstration.

The chemical mechanism used in the present study for baseline simulations is the CACM.14 CACM is based on the RADM/RACM work of Stockwell et al.37 and Jenkin et al.38 and on SAPRC-97 and SAPRC-99 (available from W.P.L. Carter at http://pah.cert.ucr.edu/~carter/). CACM

Table 2. Main features of three different photochemical mechanisms: CBM-IV, SAPRC-99, and CACM.

Feature	CBM-IV	SAPRC-99	CACM	
No. reactions	81	237	361	
No. species	33	72	191	
No. organics	11	39	129	

includes O_3 chemistry, a comprehensively resolved treatment of VOC oxidation and chemistry of SOA precursors. The model is composed of 361 chemical reactions and 191 gas-phase species: 120 fully integrated species, 67 pseudosteady-state species, and 4 species that have fixed concentration.

Jimenez et al. 13 conducted a comparison among various chemical mechanisms including SAPRC-99, CB-IV, and CACM (Table 2). The comparison was based on box model simulations of remote atmosphere conditions. Neither emissions nor deposition were considered. It is difficult to determine which mechanism more accurately represents real atmospheric conditions. Measurements from smog chamber experiments could be used to discriminate between mechanisms, but these experiments only represent limited chemical systems and can be affected by experimental uncertainties. Jimenez et al.¹³ based their comparison on the average values using all of the mechanisms. One limitation of this approach is that comparisons are based on only one set of ICs. Simulations in three-dimensional models usually start from a large set of ICs and interactions between and among model cells that might lead to different results from the comparisons.

Jimenez et al.¹³ reported that CACM and LCC are the mechanisms that produce the highest O_3 concentration. CACM produced a difference in O_3 peak concentration of +41% with respect to the average, and LCC produced a difference of +18.2%.

When a full three-dimensional model is used to compare the chemical mechanisms in the current study, the CACM mechanism produces an O₃ peak that is higher than LCC, which is consistent with box model results in Jimenez et al. 13 Maximum O_3 concentration obtained with CACM is 258 ppb, whereas LCC produces an O₃ peak of 153 ppb. In addition, spatial distribution of O₃ concentration in each case differs significantly. These spatial effects cannot be observed with box model analyses alone. CACM produces the peak O₃ concentration over the northeastern region of the domain, at downwind locations, whereas the LCC mechanism produces the peak O₃ concentration over the east part of Riverside, closer to the main sources (Figure 1h). The difference between these cases is caused mainly by faster O₃ removal considered in the LCC mechanism. As reported in Jimenez et al., ¹³ HNO₃ concentrations produced by LCC are higher than CACM. In addition, formation of PAN is slower in CACM. As a result, PAN is transported farther downwind and, therefore, peak O₃ concentrations move toward the east. The significant differences in both magnitude and location of the O₃ peak caused by changes in chemical mechanism used in the full three-dimensional model discovered in the current work suggest that predictions are highly dependent on the chemical mechanism. Because

there is significant uncertainty in the chemical mechanism and disagreement in the community with regard to which mechanisms represents reality more accurately, the use of more than one of the accepted chemical mechanisms is suggested for air quality evaluation.

COMPARISON AMONG CIT, CALGRID, AND UAM SIMULATIONS

One of the major applications of air quality modeling is to set a basis for air pollution control strategies. The SCAQMD has developed plans to reduce emissions and, hence, comply with the NAAQS. To demonstrate that the measures proposed in the AQMP produce the desired pollutant reduction, SCAQMD uses two different air quality models: (1) UAM with the CB-IV chemical mechanism, and (2) CALGRID with the SAPRC-99 chemical mechanism. This section compares different results produced by CALGRID, UAM, and the CIT airshed model. In addition to the different chemical mechanisms used, other model features are listed in Table 3. Notice that the models encompass areas of different size. The SCOS97 domain extends from 275 to 595 km UTM Easting and from 3670 to 3870 km UTM Northing. The CIT domain has a smaller size and is not completely rectangular, but extends from \sim 300 to 550 km UTM Easting and from 3700 to 3810 km UTM Northing. Because CALGRID and UAM use a domain size different than the CIT model, different boundary conditions are needed. As mentioned in previous sections, different boundary conditions are a source of discrepancies in simulation results.

Also, the vertical resolution is different in each model. The UAM and CIT models consider five vertical layers with variable height, finer resolution at ground level, and coarser resolution at the top. Although considering a larger number of vertical layers, CALGRID assumes a fixed vertical height. As a result, CALGRID provides coarser resolution than UAM and CIT at ground level.

Two main aspects that are different in the three models are the chemical mechanisms and advection solvers. UAM uses CB-IV, and CALGRID uses SAPRC-99, whereas CIT uses CACM. CB-IV has the lowest and CACM has the highest O₃ forming potential. Regarding the advection solver, UAM uses a Smolarkewicz scheme, which was found to be significantly less accurate than the Galerkin scheme and the QSTSE, used in CALGRID and CIT, respectively. Table 4 shows the maximum O₃ concentration predicted by each of these different air quality models. Among the models discussed above, CALGRID estimates the lowest peak O_3 concentration using the meteorology of August 5-6, 1997. Although UAM uses a chemical mechanism that tends to produce less O₃ and an advection solver that diffuses more pollutant concentrations than CALGRID, UAM estimates a higher peak O₃ concentration than CALGRID during the same meteorological episode. One reason for this difference is attributable to a different consideration of solar radiation and cloud cover. UAM does not consider cloud cover or radiation extinction, and, as shown previously, stronger radiation tends to produce higher O₃ concentrations (peak O₃ increases by 1 ppb because of an increase of 1% in UV radiation). Other factors, such as different deposition or vertical

Table 3. Comparison of CALGRID, UAM, and CIT modeling systems.

Parameter	CALGRID	UAM	CIT	
Modeling system				
Domain size	SCOS97	SC0S97	CIT	
Grid size	5-km	5-km	5-km	
Vertical layer structure	Fixed 16 layers	Variable 5 layers	Variable 5 layers	
Region top	5000 meters	2000 meters	1100 meters	
Boundary/top/initial conditions	Modified EPA clean	Modified EPA clean	Based on historical values	
Modeling coordinate system	Lambert conformal	UTM	UTM	
Emissions				
Emissions inventory	2010 ARB/district	2010 ARB/district	2010 ARB/district	
Chemistry				
Basic module	SAPRC-99	CB-IV	CACM	
Chemical solver	Quasi steady states analysis or hybrid solver	Quasi-steady state assumptions with Crank-Nicholson algorithm	Quasi steady states analysis or hybrid solver	
Photolysis rates	Radiation extinction as height above sea level	One-dimensional based on Zenith angle	Radiation extinction as height above sea level	
Meteorology				
Meteorological data	1987 SCAQS	1987 SCAQS	1987 SCAQS	
Wind model	MM5-4DDA	CALMET		
Advection	Chapeau function based scheme with Forester filter	Forward-upstream diffusive-corrected algorithm of Smolarkewicz	Quintic spline Taylor series expansion	
Vertical diffusivity/diffusion	Horizontal diffusion: based on stability class with adjusted wind speed, (Smagorinsky method); vertical diffusivity: combination of various methods depending on stability and layer height	Vertical diffusivity coefficient is calculated internally	Horizontal diffusion: based on stability class with adjusted wind speed, (Smagorinsky method); vertical diffusivity: combination of various methods depending on stability and layer height	
Dry deposition	Surface resistance model	Roughness length, stability, wind, speed, deposition factor	Surface Resistance model	
Mixing heights	CALMET	Holsworth	CALMET	
Cloud cover	Yes	None	None	
Mass continuity adjustment	NONR	O'Brien scheme	None	

Notes: EPA = U.S. Environmental Protection Agency; NONR = nonreactive species adjustment; ARB = California Air Resources Board; CALMET = Diagnostic 3-Dimensional Meteorological Model; MM5 = Penn State/National Center for Atmospheric Research Mesoscale Model; 4DDA = 4-Dimensional Data Assimilation.

transport (not discussed in this work), could also contribute to variations in the peak O_3 predictions. The CIT model estimates much higher peak O₃ concentrations than the other two models. The main causes of such a difference are attributable to the chemical mechanism and the advection solver, as discussed in previous sections. To further investigate this, an additional simulation is conducted using the CIT model with a chemical mechanism and advection solver that are similar to those used by CALGRID. These results are also presented in Table 4. The peak O₃ concentration obtained with this simulation is in agreement with the results obtained by CALGRID. Note that the CIT case even used a different meteorological episode than the one used in CALGRID. As a result, peak O₃ concentration estimated by CIT with LCC/Galerkin advection solver is slightly lower than the one predicted by CALGRID.

CONCLUSIONS

This work presents a systematic analysis on how different elements that constitute the CIT air quality model affect O_3 concentration estimates. Results show that simulated peak O_3 concentration is highly sensitive to meteorological conditions and particularly to temperature (peak O_3 varies by ≤ 9 ppb/°C in the most extreme regions where O_3 concentrations are already high). The high sensitivity to meteorological conditions suggests that a suite of meteorological episodes should be used for attainment demonstration purposes rather than relying on just one meteorological event.

Evaluation of model sensitivity to ICs suggests that using only 2 days of spin up time does not completely dissipate the effect of ICs in simulations of the SCAB, especially at downwind locations. Consequently, results suggest that a meteorological episode of ≥ 3 days should

Table 4. Comparison of peak 03 concentrations simulated using different air quality models.

Variable	UAM ^a	UAM ^a	CALGRID ^b	CIT	CIT with LCC/Galerkin
Episode	August 5–6, 1997	August 27–28, 1987	August 5–6, 1997	August 27–28, 1987	August 27–28, 1987
Peak O ₃ (ppb)	153	136	134	260	127

Notes: aFrom AQMP 200324; bFrom AQMP 2003, Appendix V.35

be used to minimize the effects of ICs. On the other hand, results show that boundary conditions do not significantly impact peak O₃ concentrations, although they affect O₃ concentrations in the central part of the domain and in locations near inflow boundaries. In addition, as suggested by previous studies, using clean air boundary conditions allows control of NO_X emissions to be more effective in reducing O₃ concentration than using historical boundary conditions. Hence, one must be careful in choosing boundary conditions to minimize their effects on simulated air quality impacts because of changes in emissions. One option to avoid having a strong influence of the boundary conditions on simulation results is to locate them far from the area of interest. However, this option increases computational expenses and requires a means of estimating or measuring meteorological and boundary conditions in a larger domain.

The use of two different advection solvers, Galerkin and QSTSE, affects the simulated dispersion of pollutants. In particular, Galerkin produces a solution more diffusive than QSTSE and leads typically to higher base concentrations over the central part of the domain but lower basinwide peak $\rm O_3$ concentration compared with QSTSE. Because pollution control strategies are typically focused on the basin-wide peak $\rm O_3$ concentration, diffusion because of the advection solver may affect the result of such strategies.

The present work shows that chemical mechanisms have a significant effect on air quality predictions. The two mechanisms used in this study, LCC and CACM, lead to differences in peak $\rm O_3$ concentration of 105 ppb. In addition, a different spatial distribution of $\rm O_3$ peak is directly attributable to differences in the chemical mechanisms. This encourages further research on chemical mechanisms and the use of multiple mechanisms for air quality evaluation.

Finally, CIT airshed model predictions are compared with the results obtained with other air quality models. The CIT airshed model typically predicts higher O_3 concentrations than the other two models considered: CAL-GRID and UAM. Simulation results of the CIT model, using a chemical mechanism and an advection solver similar to the one used by CALGRID, produced results similar to CALGRID predictions. This implies that the chemical mechanism and the advection solver are the elements that produce higher O₃ concentration in the CIT simulations with respect to the other models. The advection solver used in the CIT model is one of the most accurate schemes currently available. On the other hand, the CACM chemical mechanism used in the CIT model includes a very comprehensive treatment of O₃ formation and VOC oxidation paths so that SOA precursors can be predicted. Results presented above suggest that CALGRID and UAM simulations may underpredict pollutant concentration because of the use of a nonaccurate advection solver in conjunction with chemical mechanisms that tend to produce low O₃ concentrations. Nonetheless, there is significant uncertainty in chemical mechanisms and disagreement in the community with regard to which mechanisms are more accurate. Consequently, the use of more than one of the accepted chemical mechanisms for air quality evaluation is recommended.

In conclusion, several model parameters and components that affect O₃ concentrations have been studied extensively but in a somewhat isolated and often simplified manner. This work examines the compounding effects and sensitivity of O_3 predictions to various model parameters and components in a full three-dimensional model for the year 2010 in the SCAB. Demonstration of O₃ NAAQS attainment by air quality models requires that models accepted by the scientific and regulatory communities predict a peak O₃ concentration of 120 ppb under different meteorological conditions. However, model sensitivity to inputs and to different model elements suggests that the predicted peak O₃ concentration may vary significantly from model to model depending on the model parameters and components. Uncertainty in predicted peak O₃ concentration suggests that air quality evaluation should not be based solely on this single value but also on trends predicted by air quality models using a number of chemical mechanisms and with an advection solver that is mass conservative.

ACKNOWLEDGMENTS

The authors graciously acknowledge the financial support of the California Energy Commission for sponsoring this work. Any opinions, findings, and conclusions or recommendations expressed in this material are those of the authors and do not necessarily reflect the views of the California Energy Commission. The authors thank the California Air Resources Board and SCAQMD for their provision of the emissions inventory. The authors thank Prof. G.S. Samuelsen from the Advanced Power and Energy Program, University of California Irvine, for his comments and constructive criticism. Marc Carreras thanks the Balsells-Generalitat de Catalunya Fellowship for graduate research fellowship.

REFERENCES

- Russell, A.G.; Dennis, R. NARSTO: Critical Review of Photochemical Models and Modeling; Atmos. Environ. 2000, 34, 2283-2324.
- Fine, J.; Vuilleumier, L.; Reynolds, S.; Roth, P.; Brown, N. Evaluating Uncertainties in Regional Photochemical Air Quality Modeling; *Annu. Rev. Environ. Resour.* 2003, 28, 59-106.
- 3. Harley, R.A.; Russell, A.G.; McRae, G.J.; Cass, G.R.; Seinfeld, J.H. Photochemical Modeling of the Southern California Air Quality Study; *Environ. Sci. Technol.* **1993**, *27*, 378-388.
- Reynolds, S.D.; Michaels, H.; Roth, P.; Tesche, T.W.; McNally, D.; Gardner, L.; Yarwood, G. Alternative Base Cases in Photochemical Modeling: Their Construction, Role and Value; Atmos. Environ. 1996, 30, 1977-1988.
- Kumar, N.; Russell, A.G. Comparing Prognostic and Diagnostic Meteorological Fields and Their Impacts on Photochemical Air Quality Modeling; Atmos. Environ. 1996, 30, 1989-2010.
- Hov, Ø.; Zlatev, Z.; Berkowicz, R.; Eliassen, A.; Prahm, L.P. Comparison of Numerical Techniques for Use in Air Pollution Models with Non-Linear Chemical Reactions; Atmos. Environ. 1989, 23, 967-983.
- Dabdub, D.; Seinfeld, J.H. Numerical Advective Schemes Used in Air Quality Models—Sequential and Parallel Implementation; Atmos. Environ. 1994, 28, 3369-3385.
- Winkler, S.L.; Chock, D.P. Air Quality Predictions of the Urban Airshed Model Containing Improved Advection and Chemistry Algorithms; Environ. Sci. Technol. 1996, 30, 1163-1175.
- Nguyen, K.; Dabdub, D. Two-Level Time-Marching Scheme Using Splines for Solving the Advection Equation; *Atmos. Environ.* 2001, 35, 1627-1637.
- Poppe, D.; Aumont, B.; Ervens, B.; Geiger, H.; Herrmann, H.; Roth, E.P.; Seidl, W.; Stockwell, W.R.; Vogel, B.; Wagner, S.; Weise, D. Scenarios for Modeling Multiphase Tropospheric Chemistry; *J. Atmos. Chem.* 2001, 40, 77-86.
- 11. Olson, J.; Prather, M.; Berntsen, T.; Carmichael, G.; Chatfield, R.; Connell, P.; Derwent, R.; Horowitz, L.; Jin, S.; Kanakidou, M.; Kasibhatla, P.; Kotamarthi, R.; Kuhn, M.; Law, K.; Penner, J.; Perliski, L.;

- Sillman, S.; Stordal, F.; Thompson, A.; Wild, O. Results from the Intergovernmental Panel on Climate Change (IPCC) Photochemical Model Intercomparison (PhotoComp); *J. Geophys. Res.* **1997**, *102*, 5979-5991.
- Kuhn, M.; Builtjes, P.J.H., Poppe, D.; Simpson, D.; Stockwell, W.R.; Andersson-Skold, Y.; Baart, A.; Das, M.; Fiedler, F.; Hov, O.; Kirchner, F.; Makar, P.A.; Milford, J.B.; Roemer, M.G.M., Ruhnke, R.; Strand, A.; Vogel, B.; Vogel, H. Intercomparison of the Gas-Phase Chemistry in Several Chemistry and Transport Models; *Atmos. Environ.* 1998, 32, 693-709
- Jimenez, P.; Baldasano, J.M.; Dabdub, D. Comparison of Photochemical Mechanisms for Air Quality Modeling; *Atmos. Environ.* 2003, 37, 4179-4194.
- Griffin, R.J.; Dabdub, D.; Seinfeld, J.H. Secondary Organic Aerosol—1. Atmospheric Chemical Mechanism for Production of Molecular Constituents; J. Geophys. Res. Atmos. 2002, 107, 4332.
- Zhang, Y.; Pun, B.; Vijayaraghavan, K.; Wu, S.-Y.; Seigneur, C.; Pandis, S.N.; Jacobson, M.Z.; Nenes, A.; Seinfeld, J.H. Development and Application of the Model of Aerosol Dynamics, Reaction, Ionization, and Dissolution (MADRID); *J. Geophys. Res.* 2004, 109, D01202.
- Vutukuru, S.; Grifin, R.J.; Dabdub, D. Simulation and Analysis of Secondary Organic Aerosol Dynamics in the South Coast Air Basin of California; J. Geophys. Res. Atmos. 2006, 10.1029/2005JD006139.
- 17. O'Neill, S.M.; Lamb, B.K. Intercomparison of the Community Multiscale Air Quality Model and CALGRID Using Process Analysis; *Environ. Sci. Technol.* **2005**, *39*, 5742-5753.
- 18. Griffin, R.J. Dabdub, D.; Kleeman, M.J.; Fraser, M.P.; Cass, G.R.; Seinfeld, J.H. Secondary Organic Aerosol—3. Urban/Regional Scale Model of Size- and Composition-Resolved Aerosols; *J. Geophys. Res. Atmos.* **2002**, *107*, 4334.
- Moya, M.; Pandis, S.N.; Jacobson, M.Z. Is the Size Distribution of Urban Aerosols Determined by Thermodynamic Equilibrium? An Application to Southern California; *Atmos. Environ.* 2002, *36*, 2349-2365.
- Knipping, E.M.; Dabdub, D. Modeling Surface-Mediated Renoxification of the Atmosphere via Reaction of Gaseous Nitric Oxide with Deposited Nitric Acid; Atmos. Environ. 2002, 36, 5741-5748.
- Meng, Z.Y.; Dabdub, D.; Seinfeld, J.H. Size-Resolved and Chemically Resolved Model of Atmospheric Aerosol Dynamics; *J. Geophys. Res.* Atmos. 1998, 103, 3419-3435.
- Zeldin, M.D.; Bregman, L.D.; Horie, Y.A. Meteorological and Air Quality Assessment of the Representativeness of the 1987 SCAQS Intensive Days. Final Report to the South Coast Air Quality Management District: Diamond Bar, CA, 1990.
- Preview of the Proposed 2003 Air Quality Management Plan for the South Coast Air Basin. South Coast Air Quality Management District, January 2003.
- 24. Air Quality Management Plan 2003. Available at: http://www.aqmd.gov/aqmp/AQMD03AQMP.htm (accessed 2005).
- Bärtsch-Ritter, N.; Keller, J.; Dommen, J.; Prévôt, S.H. Effects of Various Meteorological Conditions and Spatial Emission Resolutions on the Ozone Concentration & ROG/NO_X Limitation in the Milan Area (I); Atmos. Chem Phys. Discuss. 2003, 3, 733-768.
- Sillman, S.; Samson P.J. Impact of Temperature on Oxidant Photochemistry in Urban, Polluted Rural and Remote Environments; J. Geophys. Res. Atmos. 1995, 100, 11497-11508.
- Vuilleumier, L.; Harley, R.A.; Brown, N.J.; Slusser, J.R.; Kolinski, D.; Bigelow, D.S. Variability in Ultraviolet Total Optical Depth during the Southern California Ozone Study (SCOS97); Atmos. Environ. 2001, 35, 1111-1122.
- 28. Sistla, G.; Zhou, N.; Hao, W.; Ku, J.Y.; Rao, S.T.; Bornstein, R.; Freedman, F.; Thunis, P. Effects of Uncertainties in Meteorological Inputs

- on Urban Airshed Model Predictions and Ozone Control Strategies; *Atmos. Environ.* **1996**, *30*, 2011-2055.
- 29. Li, Y.; Dennis, R.L.; Tonnesen, G.S.; Pleim, J.E. Effects of Uncertainty in Meteorological Inputs on O₃ Concentration, O₃ Production Efficiency, and O₃ Sensitivity to Emissions Reductions in the Regional Acid Deposition Modeling. In: Preprints of the 10th Joint Conference on the Applications of Air Pollution Meteorology with A&WMA, Phoenix, AZ, January 11–16, 1998; Paper no. 9A.14, American Meteorological Society: Boston. MA. 1998: pp 529-533.
- ety: Boston, MA, 1998; pp 529-533.

 30. Dabdub, D.; DeHaan, L.L.; Seinfeld, J.H. Analysis of Ozone in the San Joaquin Valley of California; *Atmos. Environ.* **1999**, *33*, 2501-2514.
- Winner, A.D.; Cass, G.R.; Harley, R.A. Effect of Alternative Boundary Conditions on Predicted Ozone Control Strategy Performance: A Case Study in the Los Angeles Area; Atmos. Environ. 1995, 29, 3451-3464.
- Benkovitz, C.M.; Berkowitz, C.M.; Easter, R.C.; Nemesure, S.; Wagener, R.; Schwarz S.E. Sulfate over the North Atlantic and Adjacent Continental Regions: Evaluation for October and November 1986 Using a Three-Dimensional Model Driven by Observation-Derived Meteorology. J. Geophys. Res. Atmos. 1994, 99, 20725-20756.
- 33. Chock, D.P. A Comparison of Numerical Methods for Solving the Advection Equation—III; *Atmos. Environ.* **1991**, *19*, 571-586.
- Attachment to the Air Quality Management Plan 2003. Available at: http://www.aqmd.gov/aqmp/docs/2003AQMD_AppV_CalGrid.pdf (accessed 2005).
- Chock, D.P.; Winkler, S.L.A. Comparison of Advective Algorithms Coupled With Chemistry; Atmos. Environ. 1994, 28, 2659-2676.
- Atkinson, R. Atmospheric Chemistry of VOCs and NOx; Atmos. Environ. 2000, 34, 2063-2101.
- Stockwell, W.R.; Kirchner, F.; Kuhn, M.; Seefeld, S. A New Mechanism for Regional Atmospheric Chemistry Modeling; *J. Geophys. Res. Atmos.* 1997, 102, 25847-25879.
- Jenkin, M.E.; Saunders, S.M.; Pilling, M.J. The Tropospheric Degradation of Volatile Organic Compounds—a Protocol for Mechanism Development; *Atmos. Environ.* 1997, 31, 81-104.

About the Authors

Marc Carreras-Sospedra is a graduate student in mechanical and aerospace engineering at the University of California, Irvine, CA. Donald Dabdub is a professor of mechanical and aerospace engineering at the University of California, Irvine, CA. Marco Rodríguez is a research scientist with the Cooperative Institute for Research in the Atmosphere (CIRA) at Colorado State University. Jacob Brouwer is an adjunct assistant professor of mechanical and aerospace engineering at the University of California, Irvine, CA, and an associate director at the National Fuel Cell Research Center. Address correspondence to: Donald Dabdub, Ph.D., Professor, Mechanical and Aerospace Engineering, University of California, Irvine, Irvine, CA 92697-3975; phone: +1-949-824-6126; fax: +1-949-824-8585; e-mail: ddabdub@uci.edu.